ChemComm

COMMUNICATION

View Article Online
View Journal | View Issue

Cite this: *Chem. Commun.*, 2023, **59**, 567

Received 22nd November 2022,
Accepted 12th December 2022

DOI: 10.1039/d2cc06317d

rsc.li/chemcomm

Cascade energy transfer augmented circular polarization in photofluorochromic cholesteric texture†

Chao Ren, Tonghan Zhao, * Yonghong Shi and Pengfei Duan *

Circularly polarized luminescence (CPL)-active light-harvesting systems consisting of a light-responsive donor (*R*-1), mediator (Nile red), and terminal acceptor (Cyanine 5) are constructed in cholesteric liquid crystals. A dynamically tunable CPL dissymmetry factor and energy transfer modes, are achieved *via* the closed-ring and open-ring conversion between *R*-1-O and *R*-1-C.

Photosynthesis, the source of food, energy, and oxygen for all people and animals, is initiated by light-harvesting antenna complexes that capture sunlight and funnel excitation energy to reaction centers along several aligned chromophores.[1] The excitation energy is generally transferred in the chiral environment formed by enzymes and other natural structures.[2] Inspired by nature, many artificial chiral light-harvesting systems based on ordered chromophore arrays have been designed.[3] Recently, these mimics with circularly polarized luminescence (CPL) properties have received increasing attention due to their unique optical properties and broad application prospects in optoelectronic devices,[4] information encryption,[5] chiral recognition,[6] and asymmetric catalysis.[7] Notably, the luminescence dissymmetry factor (g_{lum}), which defines the emission difference of left- and right-handed circularly polarized light, is one of the key performance indicators for real applications.[8]

In CPL-active light-harvesting systems, the Förster resonance energy transfer (FRET) has been demonstrated as a significant process to amplify the g_{lum} value.[9] To date, some examples of FRET-amplified CPL systems have been reported.[10] Nevertheless, rarely have studies specifically evaluated the effect of cascade energy transfer (CET) on CPL. In nature, light-harvesting processes are multi-step sequential energy transfer processes.[11] In addition, the functions of many biological light-harvesting tissues are dynamically tunable, guaranteeing smooth progress of vital functions.[12] Therefore, establishing a CET system with switchable CPL performance is appealing to simulate natural light-harvesting antennas better and gain a deeper understanding of their communication.

Here, we design a light-harvesting antenna in a cholesteric superstructure, which is dynamically changeable in response to light, to study the cooperative chirality and cascade energy transfer. Generally, nematic liquid crystals doped with chiral molecules can present a regular helical superstructure, *i.e.*, cholesteric liquid crystals (CLCs).[13] Moreover, the helical superstructure of CLCs is highly sensitive to external stimuli resulting in valuable regulation of CPL behavior.[14] As shown in Fig. 1, cholesteric liquid crystals loaded with closed-form chiral diarylethene derivatives (*R*-**1**-C) exhibit a self-organized helical superstructure. When Nile red (NR) and Cyanine 5 (Cy5) are involved in this cholesteric superstructure, the chirality of the superstructure can transfer to these achiral dyes, and the excited energy is orderly transferred in the chiral environment. In addition, the CPL assigned to the acceptor in different chiral environments could be amplified step by step through the

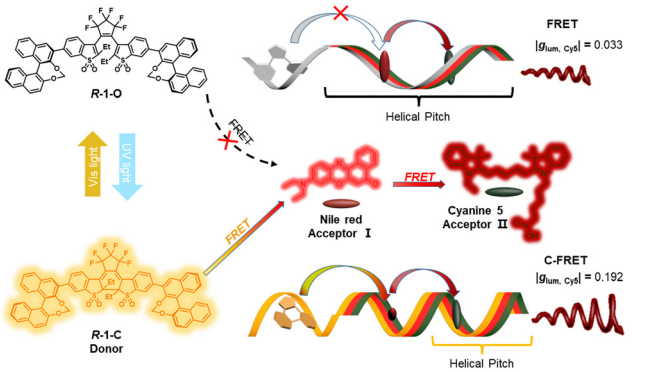

Fig. 1 Schematic representation of isomerization of *R*-**1** dynamically regulates cascaded energy transfer from the cholesteric texture. Ultraviolet light and visible light irradiation can change the molecular structure of chiral dopants and cause a change in the pitch of the cholesteric phase.

CAS Key Laboratory of Nanosystem and Hierarchical Fabrication, National Center for Nanoscience and Technology (NCNST), No. 11, ZhongGuanCun BeiYiTiao, Beijing 100190, P. R. China. E-mail: zhaoth@nanoctr.cn, duanpf@nanoctr.cn

† Electronic supplementary information (ESI) available. See DOI: https://doi.org/10.1039/d2cc06317d

energy transfer process. Therefore, the synergistic effect between chirality and sequential energy transfer is elucidated, which will contribute to better understanding of natural multi-channel information communication and light-harvesting antennas.

The synthesis of *R*(*S*)-**1** and the photoswitchable properties of *R*(*S*)-**1**, have been previously reported.[15] The chemical structures, detailed synthesis process, and characterization are described in the ESI† (Fig. S1, S2, and Table S1). We recorded the UV-Vis absorption and fluorescence spectra when the *R*-**1** solution was alternatively irradiated with 365 nm UV light and 465 nm LED (Fig. S3, ESI†). The spectra gradually changed with the illumination time of regulated light. These optical switching reactions can be repeated by alternating 365 nm and 465 nm irradiation with no appreciable alteration of the absorption and emission intensities after several cycles.

The chiroptical properties of *R*(*S*)-**1** have been confirmed *via* circular dichroism (CD) and CPL spectra measurements. As shown in Fig. S4a (ESI†), *R*-**1**-C had obvious CD signals in the UV and visible regions. This result suggests that the covalent bond of *R*-**1**-C connecting two chromophores, resulted in the transfer of chirality from the dinaphthalene part to the diarylethene. Additionally, CPL with small $|g_{lum}|$ values around 1.7×10^{-4} from *R*(*S*)-**1**-C were also obtained (Fig. S4b, ESI†), which appeared following the turn-on mode fluorescence.

There were only weak chiral signals in the solution system. Loading the chiral chromophores into the achiral nematic liquid crystals was considered as a reasonable method to enhance the value of g_{lum}.[16] Different concentrations of *R*-**1** were doped into the commercially available achiral room-temperature nematic liquid crystal (E7, Scheme S2, ESI†). When the mixing weight ratio of *R*-**1**-C/E7 was 0.5 wt%, the highest g_{lum} value was obtained, indicating that the chiral nematic liquid crystal had the most favorable configuration in this case (Fig. 2a). The dropping of the g_{lum} value at higher doping ratio resulted from the aggregation of *R*-**1**-C (Fig. S5, ESI†). The finger-printed and planar textures of *R*-**1**/E7 were observed in the liquid crystal cell employing a microscope (Fig. 2b and Fig. S6, ESI†). Typically, the chiral texture indicated that *R*-**1** induced the liquid crystal to form a cholesteric texture presenting a regular helical superstructure with large g_{lum} values. Under polarizing optical microscopy (POM), the texture of the sample in the wedge-shaped cell was observed. Unlike in a liquid crystal cell of uniform thickness, there was an angle (θ, $\tan\theta = 0.0183$) between two planes. Based on Cano's method, when the N*-LC was inserted into a wedge-shaped cell with a gradient thickness, a different number of helical pitches emerge as discontinuous lines on the surface of the liquid crystal cell, named Cano lines (Fig. 2c and d). The helical pitch (p) was calculated in line with the distance (a) between Cano lines using the following equation:

$$p = 2a\tan\theta$$

Further, the helical twisting power (HTP, β_M) was evaluated as follows:

$$\beta_M = 1/(pcr)$$

where p is the helical pitch previously calculated, c is the molar concentration percentage of the *R*-**1**, and r is the enantiomeric purity (0.99).[17] The HTP of *R*-**1**-O/E7 and *R*-**1**-C/E7 was computed to be around 14.8 μm^{-1} and 36.4 μm^{-1}, respectively. This pair of isomers of chiral dopants with distinct HTP allowed for the development of dynamically tunable light-harvesting systems.

R-**1** was used as a chiral dopant, and two achiral organic dyes – NR and Cy5, were selected for incorporation into the liquid crystals to form a cholesteric superstructure. Different chromophore S1 state energy levels must match each other to satisfy FRET conditions. As reflected in the spectral diagram, the absorption spectrum of the acceptor should overlap with the emission spectrum of the donor. As shown in Fig. S7a (ESI†), *R*-**1**-O/E7 exhibited weak absorption and no fluorescence emission in the visible region. *R*-**1**-C/E7 showed an apparent absorption peak in the visible region and a fluorescence peak with a maximum emission at 550 nm, which was located in the absorption range of the NR. Therefore, NR may be an outstanding acceptor for *R*-**1**-C in the closed-loop state. Furthermore, the emission maximum of NR was located right in the absorption range of Cy5, making it possible to act as an energy mediator in the light-collecting system (Fig. S7b and S8, ESI†). These results suggest that these chromophores have matching energy levels (Fig. S9, ESI†), allowing efficient FRET to occur (Fig. S10, ESI†).

Adding different amounts of NR to the cholesteric texture of *R*-**1**-C/E7, we observed that the emission at 550 nm decreased, and a new emission around 620 nm from NR appeared and enhanced with the increasing amount of NR. These results indicated that NR could act as a receptor of *R*-**1**-C for efficient energy transfer. When the mass ratio of *R*-**1** to NR was 10 : 1, the emission of NR reached the optimal state. Further, increasing the amount of NR led to quenching of the emission due to molecular aggregation (Fig. S7c, ESI†). When a second acceptor, Cy5, was added under this condition, the emission attributed to NR decreased. In contrast, a new emission from Cy5 around 700 nm appeared

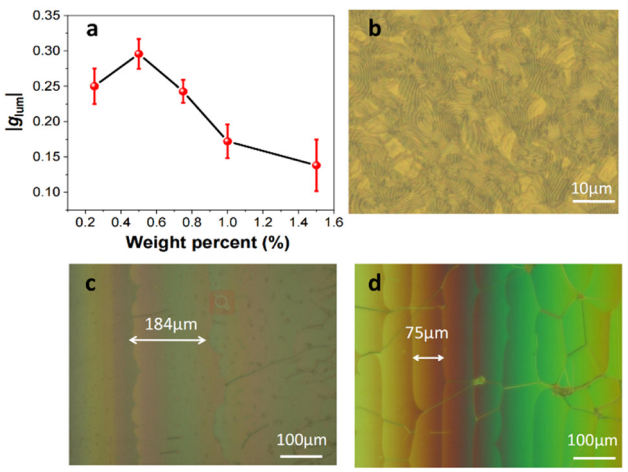

Fig. 2 (a) The tendency of CPL g_{lum} values with different mixing weight ratios of *R*-**1**-C, λ_{ex} = 360 nm, all error bars show the mean ± standard deviation, n = 5 independent experiments. (b) POM image of *R*-**1**-C/E7, [*R*-**1**-C] = 0.5 wt%. POM images of N*-LC including 0.5 wt% (c) *R*-**1**-O and (d) *R*-**1**-C in wedge-shaped cells at room temperature.

(Fig. S7d, ESI†). When the ratio of *R*-**1**/NR/Cy5 was 20 : 2 : 1, the emission of Cy5 reached the highest intensity. Therefore, the E7/*R*-**1**/NR/Cy5 with ratio 4000 : 20 : 2 : 1 was used for subsequent experiments. These results indicate that the light-harvesting system constructed by the ordered chromophore *R*-**1**-C/NR/Cy5 in the liquid crystals could effectively guide the excitation energy to the terminated acceptor. Time-resolved measurements were performed to further illustrate the energy transfer process and to reveal the possible mechanism (Fig. S11, ESI†). Compared with the *R*-**1**-C doped cholesteric texture, the average lifetime of donor *R*-**1**-C in the *R*-**1**-C/NR and *R*-**1**-C/NR/Cy5 co-doped cholesteric texture is sequentially shortened. The shortened emission decay time of donor *R*-**1**-C suggested that the energy transfer between these ordered chromophores mainly followed the Förster resonance mechanism. These created a precondition for the progressive amplification of the CPL attributable to acceptors.[18]

The chirality of the cholesteric phase shows anisotropy, and the cholesteric CD is often called liquid crystal-induced circular dichroism (LCICD).[19] The periodic structure of cholesteric texture produces Bragg reflections of light.[20] The mechanism of CPL in N*LCs can be classified into two categories: the first case is the Bragg reflex, the other is optical rotation.[21] In this work, N*LCs induced by chiral emitters should be assigned to the latter LCICD of the oriented cholesteric phase with a rotationally symmetric orientation distribution about the direction parallel to the optical axis of the light source, can be measured.[22] Therefore, we tested the LCICD of the formed cholesteric texture. As shown in Fig. 3a, the cholesteric texture with the chiral dopant exhibited obvious LCICD. When NR or Cy5 was used as the dopant to form the cholesteric texture, the CD spectra showed that the chiroptical response assigned to the *R*(*S*)-**1** moiety remained and a new signal assigned to the new acceptor appeared (Fig. 3b and c). When E7/*R*(*S*)-**1**/NR/Cy5 formed the cholesteric texture together, the LCICD of both acceptors could be observed (Fig. 3d).

The *R*(*S*)-**1**-doped cholesteric structure could respond to various external stimuli (Fig. S12–S14, ESI†), accordingly creating the necessary conditions to explore the characteristics of the excited energy transmission in the chiral environment. The CPL of *R*(*S*)-**1**-C/NR and *R*(*S*)-**1**-C/NR/Cy5 doped cholesteric texture were measured. In the system composed of *R*(*S*)-**1**/NR (Fig. S15a, ESI†), the donor's fluorescence of open-ring and close-ring states determined whether the excitation energy could be effectively transferred to the acceptor. *R*(*S*)-**1**-C served as an excellent donor to transfer ultraviolet excitation to NR, while the emission of *R*(*S*)-**1**-O no longer existed, prohibiting this energy transfer (Fig. S15b, ESI†). The cholesteric texture of individual *R*(*S*)-**1**-C-dopants showed a CPL at 550 nm. After mixing with NR, the CPL peak of the cholesteric texture shifted to 620 nm, and the original CPL signal became concurrently nondetectable. This result showed that the excited-state energy from *R*(*S*)-**1**-C was collected by NR and emitted a new CPL signal. On the other hand, the donors in the *R*(*S*)-**1**-O/NR-doped system were non-fluorescent during energy transfer. The trace amount of NR could be directly excited by a non-polarized light source longer than 470 nm. A weak CPL was recorded. The small helical twisting force provided by *R*-**1**-O made the *R*-**1**-O/NR-doped cholesteric texture form a relatively weak chiral environment. These results indicate that in the system composed of *R*(*S*)-**1**/NR, when UV light is intense, the donor *R*(*S*)-**1** captures the energy and transfers it to NR, resulting in intense CPL. More importantly, this CPL is larger than the CPL produced by directly primed receptors. When the environment changes, more intense visible light makes the antenna system exhibit a small environment, and NR directly captures energy to produce weak CPL (Fig. S15c, ESI†).

Subsequently, the CPL assigned to the receptor Cy5 was studied in the cholesteric texture formed by the three chromophores, *i.e.*, E7/*R*(*S*)-**1**/NR/Cy5. The fluorescence (550 nm) of *R*(*S*)-**1**-C almost completely disappeared, and a weak residual fluorescence (600 nm) of NR could be observed due to the sequential energy transfer. In the system of the close-ring state of the chiral dopant *R*(*S*)-**1**, a weaker CPL is obtained at 700 nm upon direct excitation of the acceptor Cy5 at 625 nm, g_{lum} = +0.071/−0.081. When the intermediate donor NR was excited (λ_{ex} = 550 nm), a significantly amplified CPL signal from Cy5 was measured, g_{lum} = +0.135/−0.158. Further excitation of the donor *R*(*S*)-**1**-C using 360 nm irradiation also produced a CPL in the emissive region of Cy5 with a g_{lum} = +0.181/−0.192, again enhanced compared to excitation of the intermediate donor NR (Fig. 4a–c). This suggests that achiral receptors not only capture the chirality conferred by the cholesteric environment but can also be induced to generate CPL. Furthermore, the CPL ascribed to the acceptor could be sequentially amplified through cascade energy transfer through the ordered chromophore arrangement (Fig. 4d). These results show that the system composed of *R*(*S*)-**1**-C/NR/Cy5 dynamically captures ultraviolet or visible light and transmits the excitation energy in different chiral environments, simulating the natural optical capture antenna.

Combined with the experimental results of this work, the possible mechanism of CPL amplification from the CET process was proposed. As shown in Fig. S8b (ESI†), CPL with a g_{lum} value of about 0.3 was obtained when the *R*-**1** doped choleric

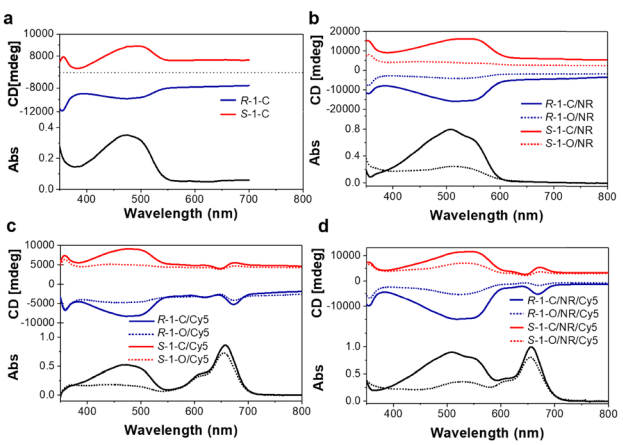

Fig. 3 CD spectra of cholesteric texture from (a) *R*-**1**-C and *S*-**1**-C, (b) *R*-**1**-C/NR, *R*-**1**-O/NR, *S*-**1**-C/NR, and *S*-**1**-O/NR, (c) *R*-**1**-C/Cy5, *R*-**1**-O/Cy5, *S*-**1**-C/Cy5, and *S*-**1**-O/Cy5, and (d) *R*-**1**-C/NR/Cy5, *R*-**1**-O/NR/Cy5, *S*-**1**-C/NR/Cy5 and *S*-**1**-O/NR/Cy5.

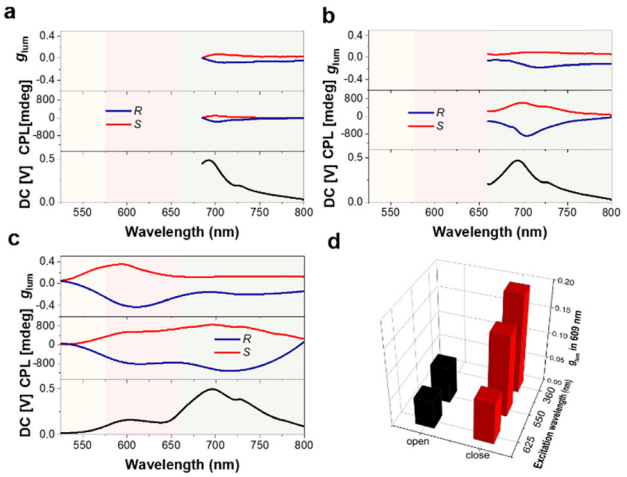

Fig. 4 (a–c) CPL spectra of *R*(*S*)-**1**-C-NR-Cy5 cholesteric texture (λ_{ex} = 625 nm, λ_{ex} = 550 nm, λ_{ex} = 360 nm, respectively). (d) 3D Column diagrams of CPL g_{lum} values obtained by irradiation of donor *R*-**1** or acceptor dyes when CET was turned "on" and "off", respectively.

phase was directly excited by unpolarized light. In the presence of the NR receptor, the CPL energy was transferred to the receptor, and a new CPL attributed to NR was emitted (Fig. S12b, ESI†). The helicity in fluorescence from a rotating donor dipole could be conserved after the FRET process, which has been approved in previous literature.[9] Furthermore, CPL amplified by cascade energy transfer in the second acceptor Cy5 could be described as the following process: the continuous rotation of Cy5 was involved in forming the cholesteric phase to obtain LC-induced chirality. Unpolarized light at 625 nm can directly excite anisotropic phase chiral Cy5 to produce a weak CPL. However, upon excitation of UV light (360 nm), the helical dipole transferred from *R*-**1**-C *via* NR to Cy5 accompanied cascade energy transfer. Consequently, a sequentially amplified CPL was achieved.

In summary, a light-harvesting antenna in a dynamically tunable cholesteric superstructure has been established, which could efficiently transfer chirality and energy in different chirality environments under light control. In particular, this continuous energy transfer attributed to the CPL of the acceptor Cy5 has been progressively enhanced, and the process could be turned "on" and "off" with the change of chiral environment. We revealed the synergistic effect of chiral and cascade energy transfer in dynamic environments, which provided an in-depth understanding of light-harvesting processes that occur in the kaleidoscopic chiral environment in nature.

This work was supported by the National Natural Science Foundation of China (22205045, T. Z.; 52173159 and 91856115, P. D.); the National Key Basic R&D Research Program of Ministry of Science and Technology of the People's Republic of China (2021YFA1200303, P. D.); the Strategic Priority Research Program of Chinese Academy of Sciences (XDB36000000, P. D.); the Beijing Municipal Science and Technology Commission (JQ21003, P. D.).

Conflicts of interest

The authors declare no conflict of interest.

Notes and references

1 (*a*) J. Barber, *Chem. Soc. Rev.*, 2009, **38**, 185–196; (*b*) R. J. Cogdell, A. Gall and J. Koehler, *Q. Rev. Biophys.*, 2006, **39**, 227–324.
2 Y. Umena, K. Kawakami, J.-R. Shen and N. Kamiya, *Nature*, 2011, **473**(7345), 55–U65.
3 (*a*) L. V. Poulikakos, P. Thureja, A. Stollmann, E. De Leo and D. J. Norris, *Nano Lett.*, 2018, **18**, 4633–4640; (*b*) Y.-X. Yuan, J.-H. Jia, Y.-P. Song, F.-Y. Ye, Y.-S. Zheng and S.-Q. Zang, *J. Am. Chem. Soc.*, 2022, **144**, 5389–5399.
4 M. Li, Y.-F. Wang, D. Zhang, L. Duan and C.-F. Chen, *Angew. Chem., Int. Ed.*, 2020, **59**, 3500–3504.
5 M. Xu, C. Ma, J. Zhou, Y. Liu, X. Wu, S. Luo, W. Li, H. Yu, Y. Wang, Z. Chen, J. Li and S. Liu, *J. Mater. Chem. C*, 2019, **7**, 13794–13802.
6 (*a*) Y. Imai, Y. Nakano, T. Kawai and J. Yuasa, *Angew. Chem., Int. Ed.*, 2018, **57**, 8973–8978; (*b*) Y. Yang, R. C. da Costa, M. J. Fuchter and A. J. Campbell, *Nat. Photonics*, 2013, **7**, 634–638.
7 (*a*) G. Yang, Y. Y. Xu, Z. D. Zhang, L. H. Wang, X. H. He, Q. J. Zhang, C. Y. Hong and G. Zou, *Chem. Commun.*, 2017, **53**, 1735–1738; (*b*) G. Yang, L. Zhu, J. Hu, H. Xia, D. Qiu, Q. Zhang, D. Zhang and G. Zou, *Chem. – Eur. J.*, 2017, **23**, 8032–8038.
8 (*a*) Z.-L. Gong, X. Zhu, Z. Zhou, S.-W. Zhang, D. Yang, B. Zhao, Y.-P. Zhang, J. Deng, Y. Cheng, Y.-X. Zheng, S.-Q. Zang, H. Kuang, P. Duan, M. Yuan, C.-F. Chen, Y. S. Zhao, Y.-W. Zhong, B. Z. Tang and M. Liu, *Sci. China: Chem.*, 2021, **64**, 2060–2104; (*b*) P. Li, L. Li, K.-J. Jeong, X. Yu, X. Yu and Y. Xu, *Adv. Opt. Mater.*, 2022, **10**, 2102616.
9 K. Yao, Y. Li, Y. Shen, Y. Quan and Y. Cheng, *J. Mater. Chem. C*, 2021, **9**, 12590–12595.
10 K. Yao, Y. Shen, Y. Li, X. Li, Y. Quan and Y. Cheng, *J. Phys. Chem. Lett.*, 2021, **12**, 598–603.
11 L. Ji, Y. Sang, G. Ouyang, D. Yang, P. Duan, Y. Jiang and M. Liu, *Angew. Chem., Int. Ed.*, 2019, **58**, 844–848.
12 Y.-C. Cheng and G. R. Fleming, *Annu. Rev. Phys. Chem.*, 2009, **60**, 241–262.
13 (*a*) K. Akagi, *Chem. Rev.*, 2009, **109**, 5354–5401; (*b*) H. Zhang, X. Chang, C. Ma, G. Huang, B. S. Li and B. Z. Tang, *ACS Appl. Mater. Interfaces*, 2022, **14**, 43926–43936.
14 (*a*) Y. He, S. Zhang, H. K. Bisoyi, J. Qiao, H. Chen, J. Gao, J. Guo and Q. Li, *Angew. Chem., Int. Ed.*, 2021, **60**, 27158–27163; (*b*) J. Li, H. K. Bisoyi, S. Lin, J. Guo and Q. Li, *Angew. Chem., Int. Ed.*, 2019, **58**, 16052–16056; (*c*) X. Li, Y. Shen, K. Liu, Y. Quan and Y. Cheng, *Mater. Chem. Front.*, 2020, **4**, 2954–2961.
15 S. Y. Lin, S. S. Zeng, Z. Y. Li, Q. Y. Fan and J. B. Guo, *ACS Appl. Mater. Interfaces*, 2022, **14**, 30362–30370.
16 (*a*) X. Li, W. Hu, Y. Wang, Y. Quan and Y. Cheng, *Chem. Commun.*, 2019, **55**, 5179–5182; (*b*) Q. Xia, L. Meng, T. He, G. Huang, B. S. Li and B. Z. Tang, *ACS Nano*, 2021, **15**, 4956–4966; (*c*) J. Qiao, Y. He, S. Lin, Q. Fan and J. Guo, *J. Mater. Chem. C*, 2022, **10**, 7311–7318; (*d*) J. Qiao, S. Lin, J. Li, J. Tian and J. Guo, *Chem. Commun.*, 2019, **55**, 14590–14593; (*e*) A. Juan, H. Sun, J. Qiao and J. Guo, *Chem. Commun.*, 2020, **56**, 13649–13652; (*f*) Y. He, Q. Fan, J. Gao, H. Chen and J. Guo, *Mater. Chem. Front.*, 2022, **6**, 1844–1849; (*g*) Y. He, S. Lin, J. Guo and Q. Li, *Aggregate*, 2021, **2**(6), e141; (*h*) S. Lin, H. Sun, J. Qiao, X. Ding and J. Guo, *Adv. Opt. Mater.*, 2020, **8**, 2000107.
17 G. W. Gray and D. G. McDonnell, *Mol. Cryst. Liq. Cryst.*, 1979, **53**, 147–166.
18 A. Ajayaghosh, V. K. Praveen, C. Vijayakumar and S. J. George, *Angew. Chem., Int. Ed.*, 2007, **46**, 6260–6265.
19 J. X. Guo and D. G. Gray, *Liq. Cryst.*, 1995, **18**, 571–580.
20 J. W. Goodby, *J. Mater. Chem.*, 1991, **1**, 307–318.
21 J. Yan, F. Ota, B. A. San Jose and K. Akagi, *Adv. Funct. Mater.*, 2017, **27**, 1604529.
22 H.-G. Kuball and T. Höfer, *Chirality*, 2000, **12**, 278–286.

